Systemic Design And Control of Electric Vehicles Power Chain

Moez Hadj Kacem, Souhir Tounsi, Rafik Neji

Abstract— In this paper, we describe a method of systemic design of electric vehicles (EVs) power chain, reducing the cost of production and the energy consumption. This method rests on the choice of the structure and the components of this chain. For this purpose, we have selected a modular structure of a synchronous engine with permanent magnets and axial flux. The choice of the static converter oriented toward a two-level voltage structure and electromagnetic switches aims at increasing the reliability of the global system and eliminating the multiple inconveniences of the IGBTs. The adaptation of this low-frequency converter structure is assured by the insertion of a gearing speed amplifier . Finally, the modelling under the environment of Matlab/Simulink of the power chain validate this approach of design entirely.

Index Terms— Electric Vehicles , Design, Control, Electromagnetic switches, generating coil parameters, power chain.

I. INTRODUCTION

In this paper, we present a systemic design method of electric vehicle (EVs) chain power , taking into account several constraints such as the speed limit, the energy saving, the cost of the power chain and the reliability of the whole system. This method is based firstly on the analytical sizing of the power chain, and secondly on the analytical modeling of the electrical parameters of the electric actuator control. It takes into account the compatibility between the components of the power chain to reach the critical level of performance of the global system. This approach is based on the application of the general theorems relating to the design of electrotechnical devices. The global design model provides results relating to the manufacturing of the electric motor, converter and the mechanical transmission system [1]. These results increases the compatibility of this approach with the optimization procedures of EVs performance such as the speed limit, the autonomy, the production cost etc. This study ends with a validation study of the design approach. Indeed, the simulation of the electrical, mechanical and magnetic behavior on a global control model of this chain fully validates the design approach.

II. STRUCTURE OF THE POWER CHAIN

The structural diagram of the power chain is illustrated in figure 1 [1] and [3].

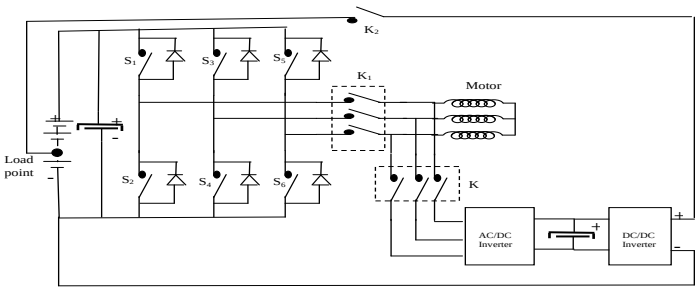

Fig. 1. Structure of the power chain

During the phases of acceleration and constant speed operation, the motor is driven by the static converter with its electromagnetic switches according trapeze control strategy which maintains the motor's phase electric current in phase with the electromotive force, which leads to a minimization of the energy consumption. In this case the switches K and K2 are open, by action of their command generating coils. However, during deceleration phases that relate to a recoverable energy, K1 is opens and K, K2 are closed and this triggers the operation of the energy recovery. In this case the motor operates as a generator. In fact, the three electromotive forces induced by the inertial force of the vehicle are transformed into a high DC voltage by an optimized DC-DC converter in order to maximize the recovered energy by the storage battery in the electric vehicle. This voltage is applied to the battery at the reload node. This node is selected in a way to maximize energy recovery [3].

III. DESIGN OF STATIC CONVERTER

A.Structure of the static converter

The static converter is an inverter that has two-level of voltage. This structure has the disadvantage of low frequency (Below 150 Hz), but it is the least expensive and does not pose the problem of floating potential, since each inverter arm is controlled by a single solenoid. on the contrary, the IGBT [4] structure offers the possibility to achieve a switching frequency of 8000 Hz which leads to a good quality of the dynamic characteristic of EVs, but it raises a lot of disadvantages among which we can cite the following:

- Energy losses leading to a reduced range of stored fixed energy
- Intervention of the capacities Trigger-Source, Trigger-Drain and Drain-Source. These capacities are involved especially at high frequencies leading to deterioration in the quality of control signals and subsequently to a degraded performance of the global traction system.
- The problem of static and dynamic Lutch-up leading to the deterioration of the general converter. In this chapter, we present only the design process of the the IEs converter because the design methods of the IGBTs are largely dealt with and presented in the literature. Another

- Moez HADJ KACEM[1,2], Souhir TOUNSI[1,2], Rafik NEJI[1,2]
- National School of Engeneers of Sfax
- (Tél : 216.74.274.088. Fax : 216.74.275.595)
- Laboratory of Electronic and Information Technology
- (LETI-Sfax) Tunisia
- kacem@yahoo.fr ; souhir.tounsi@isecs.rnu.tn ; rafik.neji@enis.rnu.tn

unstrung structure which consists in driving the movable rod by two generating coils is illustrated in Fig. 2.

This structure has the advantage of increasing the switching frequency and avoiding the maintenance problem of the springs. It may also involve several stages. It has the disadvantage of coil supply by two complementary voltages.

B. Design of the static Converter

The design parameters of the generating coil are shown in figure 3.

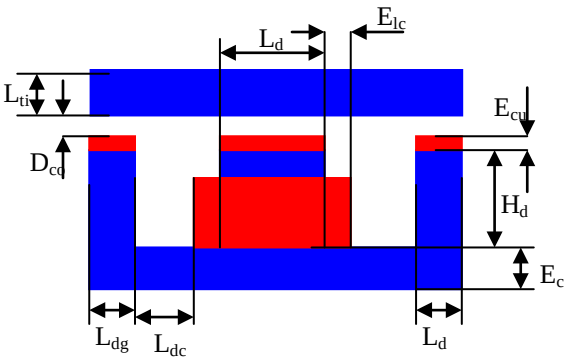

Fig. 3. Design parameters of the generating coil

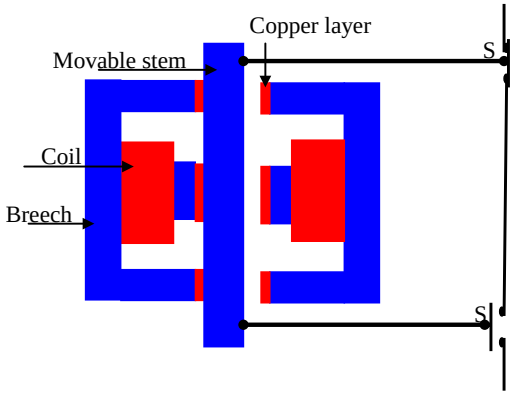

Fig. 2. Inverter arm with two generating coils

C. Dimensioning of the generating coil

The magnetic induction in copper when the rod is closed is derived from the application of Ampere's law [3, 5]:

$$B_{ec} = \mu_0 \times \mu_r \times \frac{N_{sb}^2 \times I}{2 \times E_{cu}} \quad (1)$$

Where μ_0, μ_r are respectively, vacuum, and the permeability of copper (μ_r is very close to 1), N_{sb} is the number of turns of the coil, I is in a electric current the coil and E_{cu} is the thickness of the copper layer. The width of the rod is derived from the application of the theorem of flux conservation between the tooth where the coil located rod [3,5]:

$$L_{ti} = \frac{B_{ec} \times L_d}{2 \times B_c} \quad (2)$$

Where L_d is the width of the tooth and B_c is the maximum induction in the rod. The widths of the left and right teething are given by the following two equations [3, 5]:

$$L_{dg} = \frac{B_{ec} \times L_d}{2 \times B_d} \quad (3)$$

$$L_{dd} = \frac{B_{ec} \times L_d}{2 \times B_d} \quad (4)$$

Where B_d is the induction in the left and right teeth. The thickness of the cylinder head is expressed by the following equation [3,5]:

$$E_{cs} = \frac{B_{ec} \times L_d}{2 \times B_{cs}} \quad (5)$$

The section of a main tooth is given by the following equation [3]:

$$S_d = L_d \times E_b \quad (6)$$

Where E_b is the length of the main tooth (or length of the rod).

The section of the wire depends on the maximum electric current in a steady state (I) and density of the electric current in the copper (δ):

$$S_c = \frac{I}{\delta} \quad (7)$$

The diameter of the wire is given by the following equation:

$$D_f = \sqrt{\frac{4 \times S_c}{\pi}} \quad (8)$$

The number of conductive layer is deduced by the following relationship:

$$N_{cc} = \frac{H_{db} \times f_{rc}}{D_f} \quad (9)$$

f_{rc} is where the copper filling factor and H_{db} is the height of the tooth. The number of conductors per layer is deduced by the following equation:

$$N_c = \frac{N_{sb}}{N_{cc}} \quad (10)$$

IV. DESIGN OF THE TRACTION ENGINE

A. Engine Structure

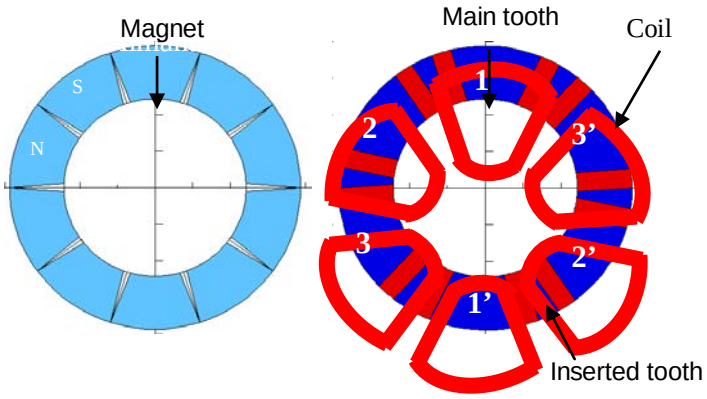

Fig. 3. Permanent magnet synchronous motor and axial flow

B. Engine design

The slot width of these structures is given by the following equation [6]:

$$L_{enc}=\left(\frac{D_e+D_i}{2}\right)\times\sin\left(\frac{1}{2}\times\left(\frac{2\times\pi}{N_d}-\alpha\times\beta\times\frac{\pi}{p}\times\left(1-r_{did}\right)\right)\right) \quad (11)$$

Where α is the report between the width of a main tooth and the width of a magnet, β is the report between a magnet and the polar step, N_d is the number of main teeth and r_{did} is the angular relation between an interposed tooth and a main tooth page. For the configurations with trapezoidal waveforms the height of a tooth is given by the following equation [6]:

$$H_d = \frac{3\times 2\times N_s}{2\times N_d}\times\frac{I_{dim}}{\delta}\times\frac{1}{K_f}\times\frac{1}{L_{enc}} \quad (12)$$

Where K_f is the filling factor of the slots, δ is the allowable current density in the slots and I_{dim} is the current size of copper conductors.

This electric current is given by the following equation [7];

$$I_{dim}=\frac{C_{dim}}{K_e} \quad (13)$$

Magnet height

$$H_a=\mu_r\times\frac{B_e}{B_r-\frac{S_d\times B_e}{S_a\times K_{fu}}}\times e \quad (14)$$

where $K_{fu} < 1$ is the coefficient of flux losses. To avoid demagnetization of the magnets, the phase electric current must be less than the demagnetization electric current Id [6]:

$$I_d=\left(\frac{B_r-B_c}{\mu_r}\times H_a-B_c\times K_{fu}\times e\right)\times\frac{p}{2\times\mu_0\times N_s} \quad (15)$$

Where B_c is the induction of demagnetization, B_r is the remanent induction of magnets and μ_0 is the permeability of air. The heights of the rotor yoke and the stator yoke are derived by applying the theorem of conservation of flow between a magnet and the rotor yoke, and between the main tooth and the stator yoke [6]:

$$H_{cr}=\frac{B_e}{B_{cr}}\times\frac{Min\left(S_d,S_a\right)}{2\times\left(\frac{D_e-D_i}{2}\right)}\times\frac{1}{K_{fu}} \quad (16)$$

$$H_{cs}=\frac{B_e}{B_{cs}}\times\frac{Min\left(S_d,S_a\right)}{2\times\left(\frac{D_e-D_i}{2}\right)} \quad (17)$$

Where B_{cr} and are B_{cs} respectively the induction in the rotor yoke and the stator yoke, S_d and S_a are respectively the section of a tooth and that of a magnet and K_{fu} is the flux leakage coefficient.

V. MODELING OF CONTROL PARAMETERS

A. DC bus voltage

The DC bus voltage is calculated in such a way that the vehicle can reach a maximum speed with a low torque undulation and without weakening. This voltage is calculated assuming that the engine runs at a stabilized maximum speed. At this operating point the electromagnetic torque to be developed by the motor is expressed by the following equation:

$$T_{Udc}=\frac{P_f}{\Omega}+C_d+\left(C_b+C_{vb}+C_{fr}\right)+\frac{C_r+C_a+C_c}{r_d} \quad (18)$$

Where P_f are the iron losses, C_d is torque due to the loss in the reducer, C_b is the torque due to the forces dry rubbing, C_{vb} is the torque duee to the viscous rubbing forces, C_{fr} is th torque due to the fluid rubbing forces, C_a is the aerodynamic torque, C_r is the torque of rolling resistance, C_c is the torque of gravity. At this operating point, the phase current of the motor is expressed by the following eclectic equation:

$$I_p=\frac{T_{Udc}}{K_e} \quad (19)$$

The electric constant is:

$$K_e=2\times n\times N_s\times\frac{\left(D_e^2-D_i^2\right)}{4}\times B_e \quad (20)$$

To reach this eclectic current value with a low ripple factor (r = 10% for example), the DC bus voltage must be a solution of the following equation:

$$r = \frac{t_m}{t_p} = 10\% \quad (21)$$

Where t_p is the time for mainting the eclectic current at a maximum speed and t_m is the time if current to increase from zero to I_d

$$t_m = -\frac{L}{R} \times \ln \left(1 - \frac{2 \times R \times I_p}{U_{dc} - K_e \times \Omega_{max}} \right) \quad (22)$$

Where R and L are respectively the resistance and inductance of the motor phase and Ω_{max} is the maximum angular velocity of the motor. The holding time of the electric current speed of a maximum (corresponding to 120 electrical degrees) is given by the following expression [2], [8] and [9]:

$$t_p = \frac{1}{3} \times \frac{2 \times \pi}{p \times \Omega_{max}} \quad (23)$$

The DC bus voltage can be deduced [2], [6] and [9]:

$$U_{dc} = \frac{2 \times R \times I_p}{1 - \exp\left(-\frac{2 \times \pi \times r}{3 \times p \times \Omega_{max} \times \frac{L}{R}} \right)} + K_e \times \Omega_{max} \quad (24)$$

B. Reduction Ratio

The insertion of a gear speed amplifier with r_d ratio aims to enable the vehicle to reach the maximum speed of 80 km / h in our application. This ratio also helps ensure proper interpolation of reference voltages in order to have a good quality of electromagnetic torque

$$r_d = \frac{R_r \times F_{ri}}{n_{qTA} \times V_{max} \times p \times n_{iTR}} \quad (25)$$

Where n_{iTR} is the reference voltages interpolation coefficient and V_{max} is the maximum speed of the vehicle.

C. Phase inductance of the motor

The leakage flux through the copper goes through about half of the copper surface, which the occurrence of the coefficient 2 in the calculation of the leakage flux reluctance in the copper. We can deduce the value of the total inductance from the following equations:

$$L = L_{fuite} + L_{entrefer} = \frac{N_s^2}{\Re_{cuivre}} + \frac{N_s^2}{+2 \times \Re_{entrefer}} \quad (26)$$

$$L = \frac{\mu_o}{2} \times \left(\frac{S_d}{e + H_a} + \frac{\left(\frac{D_e - D_i}{2} \right) \times H_d}{L_{enc}} \right) \times N_s^2 \quad (27)$$

Where L_{fuite} is the leakage inductance, $L_{entrefer}$ is the air-gap inductance S_d is the area of the main tooth, H_d is the height of the slot, H_a is the height of the magnet, L_{enc} is the width of the slot, e is the thickness of the air-gap, $\Re_{cuivre}$ is the copper reluctance and $\Re_{entrefer}$ is the copper reluctance.

D. Mutual inductance

The principle of the calculation of the mutual inductance is based on the supply of a coil for the calculation of the flux sensed by the adjacent coil. The flow path determines the total reluctance of the magnetic circuit modeling this mutual inductance. Figure 4 shows the trajectory of the flux [10] and [11].

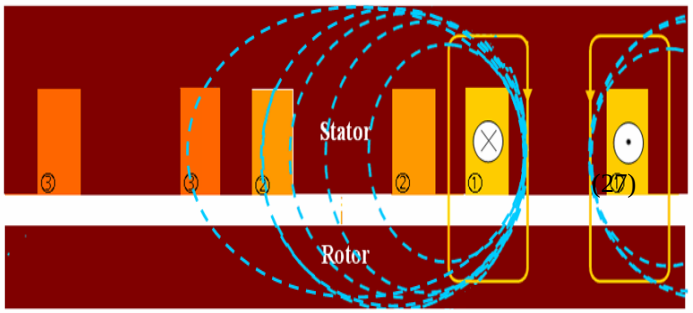

Fig. 4. Distribution of the flux generated by the coil power and captured by the adjacent coils

From Figure 5 we deduce that the reluctance network modeling the mutual inductance [10, 11].

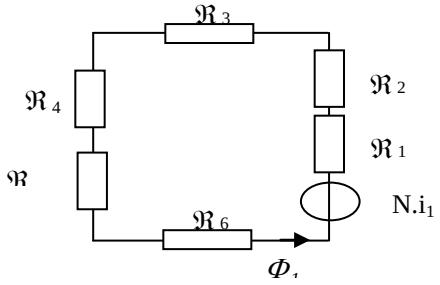

Fig. 5. Reluctance network modeling the mutual inductance

Where $\Re 1$ is the reluctance of the air-gap in front of the tooth where the coil 1 is accommodated, $\Re 2$ is the reluctance of a major tooth, $\Re 3$ is the reluctance of the stator yoke, $\Re 4$ is the reluctance of the tooth where coil $\Re 2$ is housed, $\Re 5$ is the reluctance of the air-gap in front of tooth 2 and $\Re 6$ is the reluctance of the rotor yoke. The expression of the mutual inductance is given by: :

(28)

$$M_{12} \times i_1 = N_s \times \Phi_1$$

$$M_{12} = \frac{N_s^{\,2}}{\Re} \tag{29}$$

Where Φ_1 is the flow sensed by the coil2 by supplying the coil 1, is the electric current flowing in the coil1 and $\Re$ is the total reluctance. Different mutual inductances of the motor are equal since the engine is symmetrical. It is then [10] and [11]:

$$\Re_1 = \frac{1}{\mu_0} \times \frac{2 \times (e + H_a)}{\left(\frac{D_e - D_i}{2}\right) \times \left(\frac{D_e + D_i}{4}\right) \times A_{dentm}} \tag{30}$$

$$\Re_2 = \frac{1}{\mu_0} \times \frac{2 \times H_d}{S_d} \tag{31}$$

$$\Re_3 = \frac{1}{\mu_0 \times \mu_r} \times \frac{\left(2 \times A_{encm} + \frac{3}{2} \times A_{dentm} + A_{dentim}\right) \times \frac{D_e + D_i}{4}}{H_{cs} \times \left(\frac{D_e - D_i}{2}\right)} \tag{32}$$

$$\Re_4 = \frac{1}{\mu_0} \times \frac{H_d}{S_d} \tag{33}$$

$$\Re_5 = \frac{1}{\mu_0} \times \frac{(e + H_a)}{\left(\frac{D_i - D_e}{2}\right) \times \left(\frac{D_i + D_e}{2}\right) \times A_{dentm}} \tag{34}$$

$$\Re_3 = \frac{1}{\mu_0 \times \mu_r} \times \frac{\left(2 \times A_{encm} + \frac{3}{2} \times A_{dentm} + A_{dentim}\right) \times \frac{D_e + D_i}{4}}{H_{cr} \times \left(\frac{D_e - D_i}{2}\right)} \tag{35}$$

A_{encm} where is the average width of the slot, A_{dentm} is the average width of the main tooth, A_{dentim} is the average width of the tooth interposed, H_{cr} is the height of the rotor yoke, H_{cs} is the height of the stator yoke, μ_0 is the absolute permeability, μ_r is the relative permeability of the magnets. We deduce a general expression for the mutual inductance of the motor: We deduce a general expression for the mutual inductance of the motor:

$$M_{12} = \frac{N_s^{\,2}}{(\Re_1 + \Re_2 + \Re_3 + \Re_4 + \Re_5 + \Re_6)} \tag{36}$$

E. Electromagnet inductance

The trajectory of the flux when supplying the coil is shown in figure 6 [3]:

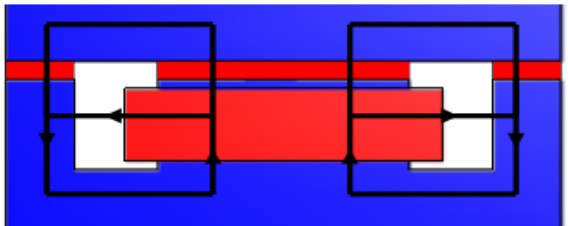

Hence, we deduce the reluctance network modeling the coil (Figure 7).

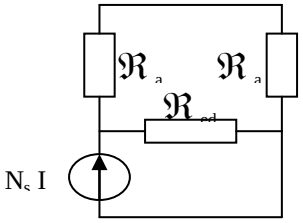

Fig. 7. Reluctance network modeling the coil

Where $\Re$ a is the reluctance of the air-gap and $\Re$ ed is the reluctance of the space between tooth From the network reluctance above, we deduce the expression of the inductance of the generating coil [3, 5]:

$$L_b = \frac{N_{sb}^2}{2 \times \Re_a} + \frac{N_{sb}^2}{\Re_{ed}} \tag{37}$$

$$\Re_a = \frac{1}{\mu_0} \times \frac{E_{cu} + D_{co} - x_t}{\frac{S_d}{2}} \tag{38}$$

Where D_{co} is the maximum aperture of the rod and xt is the displacement of the rod. Where D_{co} is the maximum aperture of the rod and xt is the displacement of the rod.

$$\Re_{ed} = \frac{1}{\mu_0} \times \frac{E_{lc} + L_{dc}}{H_{cu} \times E_b} \tag{39}$$

Where H_{cu} is the height of the coil and L_{dc} is the distance between the coil and the right tooth. Hence, we deduce the expression of the inductance of the coil [3]:

$$L_b = \mu_0 \times N_{sb}^2 \times \left(\frac{\frac{S_d}{2}}{2 \times (E_{cu} + D_{co} - x_t)} + \frac{H_{cu} \times E_b}{E_{lc} + L_{dc}} \right) \tag{40}$$

F. Attraction force of the movable rod

The attraction force of the rod derives the energy stored in the coil:

$$W_b = \frac{1}{2} \times L_b \times I^2 \tag{41}$$

This energy is transformed into mechanical energy on the side of the rod.

Hence the attraction force takes the following form:

$$F = \frac{\mu_0 \times \mu_r}{4} \times \frac{I^2 \times N_{sb}^2}{\left(E_{cu} + D_{co} - x_t\right)^2} \qquad (42)$$

VI. VALIDATION OF THE DESIGN PROCEDURE AS A WHOLE MOTOR CONVERTER

A. *Référence carrent generator*

The reference current generator allow to generate three currents of trapezoidal shapes and phase shifted relative to each other by an angle equal to 120 ° electrical. This three phase currents are out in phase with electromotive forces to minimize consumption and is amplitude controlled the speed controller. Three control loops are used to generate current in the three reference voltages of the motor. The model reference current generator is implanted under the environment of Matlab / Simulink as shown in according to the following figure 8 :

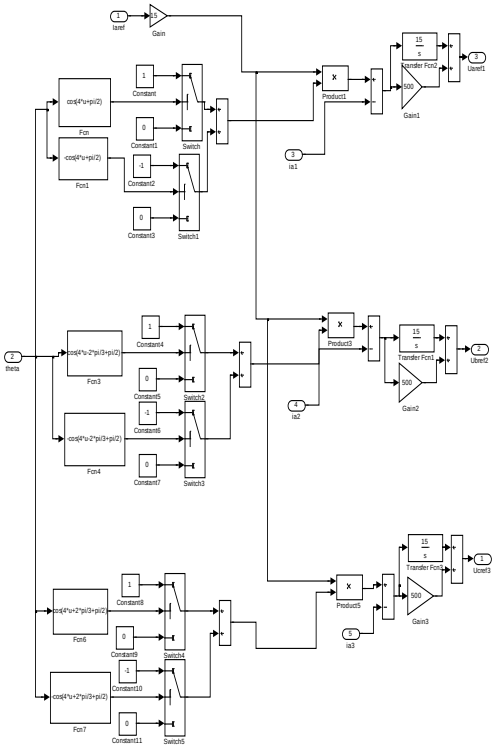

Fig. 8.Reference currents generator

B. *Converter model*

The model of the converter is based on a comparison of the three reference voltages to a triangular frequency signal much higher than these voltages. The outputs of three dial gauges attack three hysteresis to reproduce the actual shape of the voltages delivered by the converter. The model of the converter is located under the environment of Matlab / Simulink as shows in according to the following figure 9:

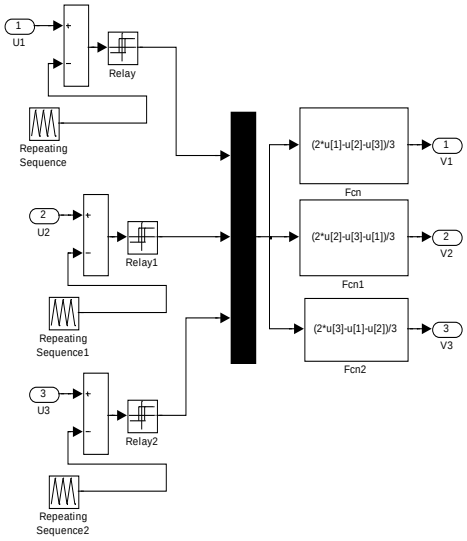

Fig. 9 .Static converter

C. *Engine Model*

The equations of phase voltages are expressed as follows:

$$u_1 = R_{t.} \times i_1 + L_t \times \frac{di_1}{dt} + e_1 \qquad (43)$$

$$u_2 = R_{t.} \times i_2 + L_t \times \frac{di}{dt} + e_2 \qquad (44)$$

$$u_3 = R_{t.} \times i_3 + L_t \times \frac{di_3}{dt} + e_3 \qquad (45)$$

$$L_t = L - M \qquad (46)$$

Where e1, e2 and e3 are respectively the electromotive forces of the phases 1, 2 and 3. The electromagnetic torque is given by the following equation:

$$T_{em} = \frac{1}{\Omega}\left(e_1 \times i_1 + e_2 \times i_2 + e_3 \times i_3\right) \qquad (47)$$

Engine model is implanted under the envireonnement Matlab / Simulink as shown in the following figure:

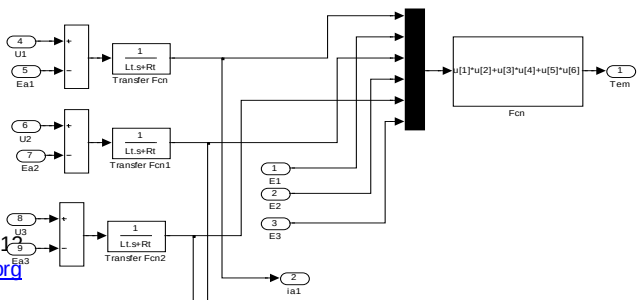

D. Equation of the vehicle movement

The equation of the vehicle motion of is derived from the fundamental relation of dynamics[12]:

$$\left(\frac{J\times r_d}{R_r}+M_v\times R_r\right)\times\frac{dv}{dt}=r_d\times C_m-(F_r+F_a+F_c)\times R_r \quad (48)$$

Where F_r is the rolling resistance force, F_a is the aerodynamic force and F_c is the gravity force.

$$F_r=f_r\times M_v\times g \quad (49)$$

$$F_a=\frac{1}{2}\times M_{va}\times C_x\times S_f\times v^2 \quad (50)$$

$$F_c=M_v\times g\times\sin(\lambda) \quad (51)$$

E. Comprehensive model of the power chain

The coupling of different models of the vehicle power chain electric leads to overall model established under the environment of Matlab / Simulink as shown in to the following figure:

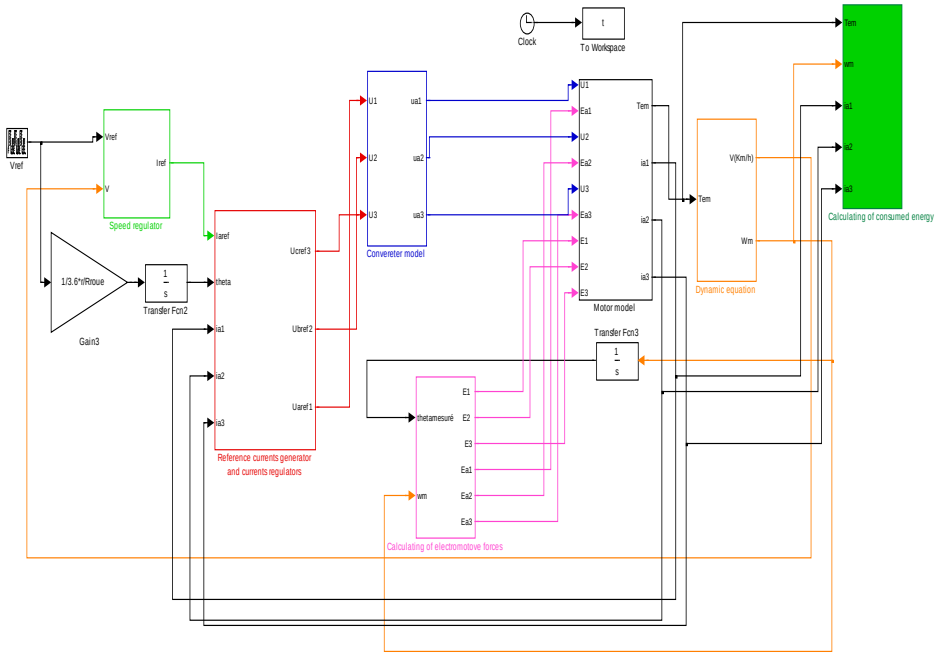

Fig. 11. Comprehensive model of the

F. F Simulation results

Figure 12 show that the speed of response precisely follows the reference speed, which shows the performance of the control technique chosen. This characteristic validates design process of the power chain.

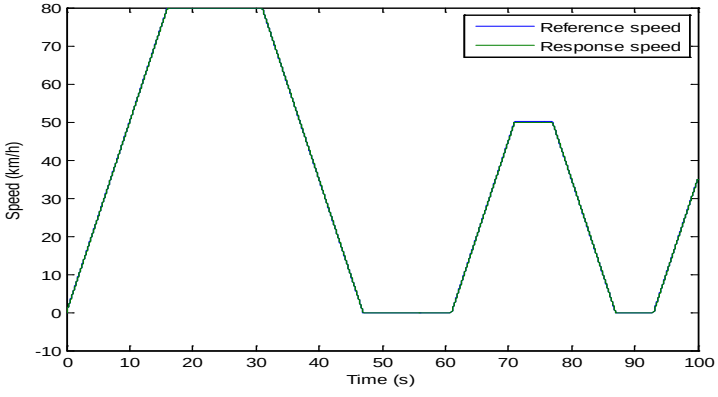

Fig. 12 Speed response

The ... re:

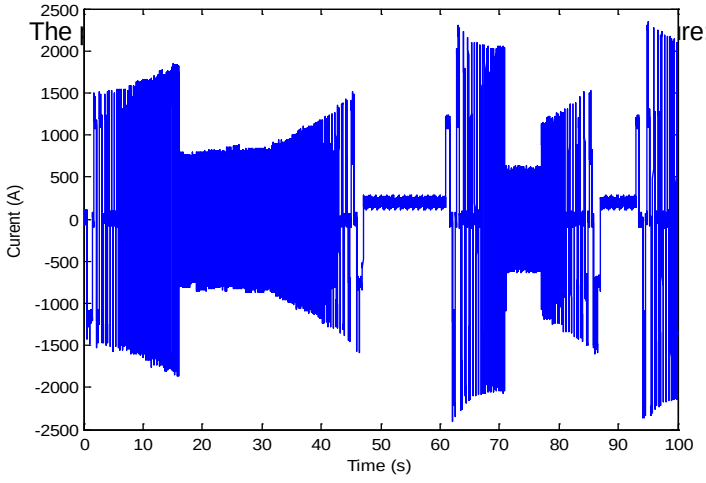

Fig. 13. The phase electric current

This figure shows that the starting electric current is greatly reduced, which leads to a reduction in energy consumption. The speed of the electric current and the phase voltage are illustrated in Figure 15 This figure shows that the electric current waveform is very close to a trapezoidal shape, which shows “once again” the performance of the control technique chosen.

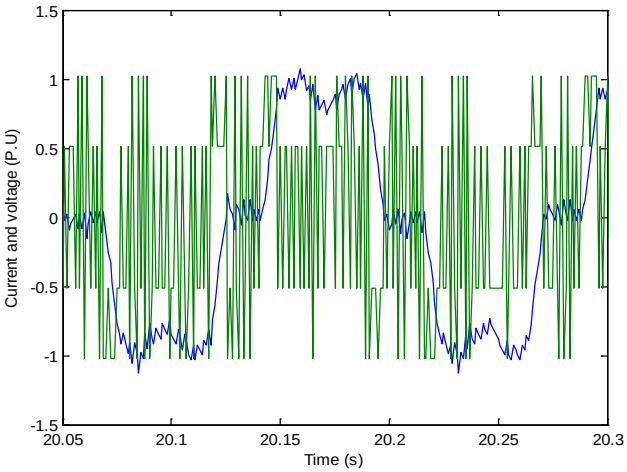

Fig. 14. Phase current and voltage.

The evolution of the electromagnetic torque is illustrated by the following figure:

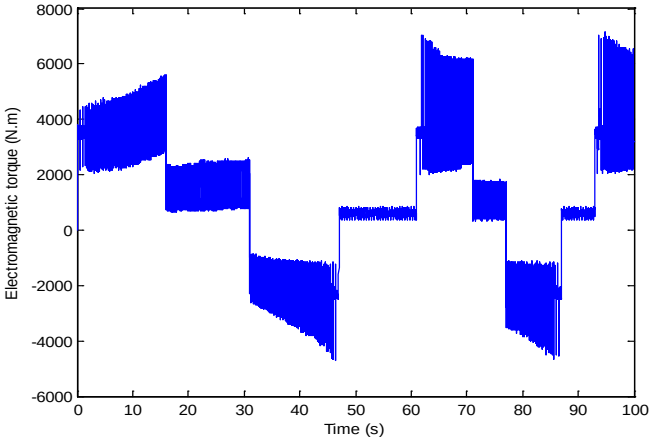

Fig. Eelectromagnetic torque.

The speed response to a standard travels is illustrated by the following figure;

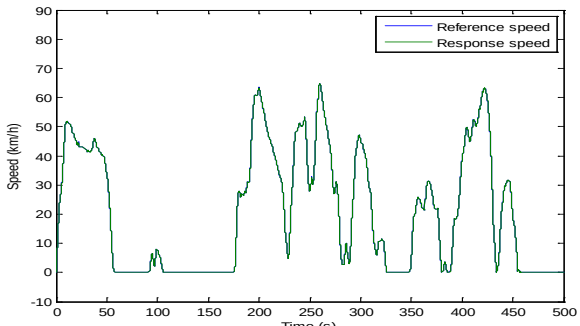

This figure shows that the response speed precisely follows the reference speed. For normalized travels energy consumption (Figure 17) is close to the average value of 0.2257 Kw.h

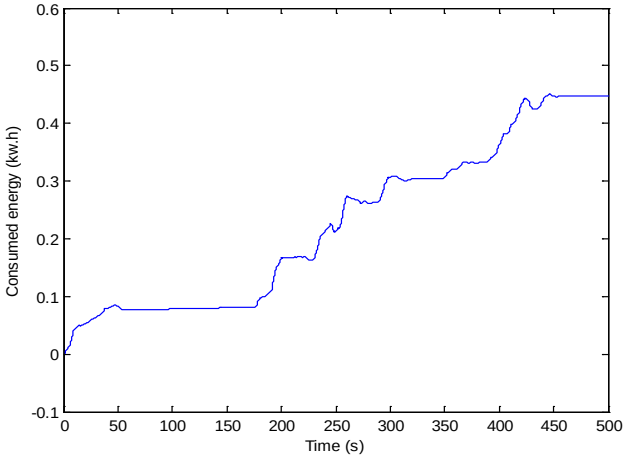

Fig. 17. Energy consumption

VII. CONCLUSION

In this paper we present a systemic design methodology of the traction electric vehicles. This methodology takes into account the interactions between the control and the design of the motor-converter. The system modeling along with a trapezoidal control law under the environment of Matlab / Simulink, validates this design approach.

REFERENCES

[1] S. TOUNSI, F. GILLON, S. BRISSET, P. BROCHET and R. NEJI: “Design of an axial flux brushless DC motor for electric vehicle,” ICEM2002 (15th International Conference on Electrical Machines), 26-8 August Bruges-Belgique, CD: ICEM02-581.

[2] S. TOUNSI and R. NEJI “Design of an Axial Flux Brushless DC Motor with Concentrated Winding for Electric Vehicles”, Journal of Electrical Engineering (JEE), Volume 10, 2010 - Edition: 2, pp. 134-146.

[3] S. TOUNSI, M. HADJ KACEM and R. NEJI: “Design of Static Converter for Electric Traction,” International Review on Modelling and Similations (IREMOS) Volume 3, N°6, December 2010, pp. 1189-1195.

[4] A. AMMOUS, B. ALLARD, H. MOREL: “Transient temperature mesurements and modeling of IGBT’s under short circuit”, IEEE transaction electronic devices, vol. 13, N°1, 1998, p. 12-25.

[5] M. HADJ KACEM, S. TOUNSI and R. NEJI: “Control of an Actuator DC Energy-saving dedicated to the Electric Traction,” International Journal of Computer Applications,” Volume 54, N° 10, September 2012, pp. 0975-8887.

[6] S. TOUNSI, "Modeling and Optimization of Engine and Battery Electric Vehicle e," Doctoral Thesis 2006, ENI Sfax.

[7] G. Ferreti, M. Gianantonio and P. Rocco, " Modelling, Identification, and compensation of pulsating torque in permanent magnet AC motors," IEEE Transactions on Industrial Electronics, Vol. 45, N°6, December 1998.

[8] S. TOUNSI, R. NEJI, and F. SELLAMI: "Design Methodology of Permanent Magnet Motors Improving Performances of Electric Vehicles," International Journal of Modelling and Simulation (IJMS), Volume 29, N° 1, 2009.

[9] N. CHAKER, I. BEN SALAH, S. TOUNSI and R. NEJI: "Design of Axial-Flux Motor for Traction Application," Journal Electromagnetic Analysis and Applications, 2009, 2, pp. 73-83.

[10] A. MOALLA, S. TOUNSI and R. NEJI: «Determination of axial flux motor electric parameters by the analytic-finite elements method», Journal of Electrical Systems, volume 4, issue 4, 2008, pp. 398-409.

[11] B. BEN SALAH, A. MOALLA, S. TOUNSI, R. NEJI et F. SELLAMI: «Analytic Design of a Permanent Magnet Synchronous Motor Dedicated to EV Traction with a Wide Range of Speed Operation», International Review of Electrical Engineering (I.R.E.E.), Volume 3, N° 1 January – February 2008.

[12] Young-Joo Lee; A. Khaligh, and A. Emadi,: " Advanced Integrated Bidirectional AC/DC and DC/DC Converter for Plug-In Hybrid Electric Vehicles", Vehicular Technology, IEEE Transactions ,Volume: 58 , N°8 ,2009 , pp: 3970 – 3980.

AUTHORS' INFORMATION

M. Hadj Kacem was born in Sfax (Tunisia) in 1975. He received his Master's diploma in Electric Engineering from the National School of Engeneers of Sfax-Tunisia in 2007. He is currently a doctorant on the Laboratory of Electronic and Information Technology (LETI-Sfax) in the National School of Engeneers of Sfax-Tunisia. His current research interests include field of electrical machines and power system design, identification, and optimisation. He is co-author of a paper in an international journal.

S. Tounsi was born in Sfax (Tunisia) in 1976. He received his Engineering Diploma, the Diplôme d'Etudes Aprofondies and the Doctorat in electrical engineering from the Ecole Nationale d'Ingénieurs de Sfax-Tunisia in 2000, 2001 and 2006 respectively. He is currently an associate professor in the Department of electrical Engineering of Electronics and Communication Superior Institute of Sfax - Tunisia (ISECS). He is a member of Laboratory of Electronic and Information Technology (LETI-Sfax). His current research interests include field of electrical machines and power system design, identification, and optimisation. He is author and co-author of more than 15 papers in international journals and of more than 30 papers published in national and international conferences.

R. Néji was born in Sfax (Tunisia) in 1958. He received his Maîtrise and the Diplôme d'Etudes Aprofondies in electrical engineering from the Ecole Normale Supérieure de l'Enseignement Technique de Tunis-Tunisia in 1983 and 1985 respectively, the Doctorat and the Habilitation Universitaire in electrical engineering from the Ecole Nationale d'Ingénieurs de Sfax-Tunisia in 1994 and 2006 respectively. He is currently a professor in the Department of Electrical Engineering of National School of Engineers of Sfax-Tunisia. He is a member of Laboratory of Electronic and Information Technology (LETI-Sfax). His current research interests include field of electrical machines and power system design, identification, and optimisation. He is author and co-author of more than 16 papers in international journals and of more than 30 papers